

# Large-aperture transparent beam steering screen based on LCMPA

HONGJUAN WANG,<sup>1</sup> OLEG YAROSHCHUK,<sup>2</sup> XIANGYU ZHANG,<sup>1</sup> ZHENFENG ZHUANG,<sup>1</sup>  
PHIL SURMAN,<sup>1</sup> XIAO WEI SUN,<sup>1</sup> AND YUANJIN ZHENG<sup>1,\*</sup>

<sup>1</sup>Luminous Advanced Displays Laboratory, School of Electrical and Electronic Engineering, Nanyang Technological University, 50 Nanyang Avenue, 639785, Singapore

<sup>2</sup>Institute of Physics of National Academy of Sciences of Ukraine, Prospect Nauky 46, 03680 Kyiv, Ukraine

\*Corresponding author: YJZHENG@ntu.edu.sg

Received 9 June 2016; revised 11 August 2016; accepted 30 August 2016; posted 30 August 2016 (Doc. ID 267850); published 23 September 2016

**A large aperture transmissive step-steering screen composed of a liquid crystal microprism array (LCMPA) deflector and a 90° twisted nematic liquid crystal (TN LC) polarization modulator is developed. The designed 3 in. (7.62 cm) device provides a steering angle of 0.95° that differs from the projected value by only 1.26% and the angular difference caused by dispersion is less than 5%. Using two-layer cascaded screens a three-direction beam steering system for stereoscopic displays is achieved with a steering step of 0.95°, undesired residual polarization contrast less than 2%, and high optical uniformity.** © 2016 Optical Society of America

**OCIS codes:** (230.3720) Liquid-crystal devices; (230.4000) Microstructure fabrication; (230.5480) Prisms; (260.1180) Crystal optics; (260.1440) Birefringence.

<http://dx.doi.org/10.1364/AO.55.007824>

## 1. INTRODUCTION

Beam steering technologies have been widely applied in many areas, such as free-space point-to-point communication in aerospace, optical tracking and sensing in projection displays, laser marking in industry, and optical switches and interconnects in telecommunications. The majority of beam steering technologies usually work with mechanically moving parts, such as MEMS-controllable microlens arrays [1] and electrostatic comb drive-actuated micromirrors [2]. These have been employed to steer laser beams in free-space optical interconnect systems and linear arrays have been used in biomedical image processes [3]. However, these systems are rather bulky, have slow speed, require a complex manufacturing process, and incorporate moving elements. To overcome these limitations, a series of nonmechanical beam steering techniques have been developed recently. For example, a dielectrophoresis-tilted prism was demonstrated by Lin in which the driving voltage and small aperture issues need to be solved [4]. Polarization gratings diffractive and active phased beam steering design methods were presented but were only suitable for narrowband wavelength [5–11]. Electrowetting microprisms were utilized to steer the beam under high operation voltages by Smith [12]. An acoustic metasurface demonstrated to fulfill the beam steering function by using tapered labyrinthine metamaterials by Xie [13].

Our research is focused on the development of a large-aperture planar step-steering screen for stereoscopic applications; it should operate in the transmissive mode, have fast

speed, and accurate beam steering angle. The device was developed for the specific purpose of steering the light output from a fast display in order to achieve spatiotemporal multiplexing for a super multiview 3D display [14]. In the proposed stereoscopic display system, the linearly polarized visible light from a monitor with the viewing angle  $\pm 30^\circ$  should be steered in the  $-0.95^\circ$  (left),  $0^\circ$  (original), and  $0.95^\circ$  (right) directions.

For the selection of the most suitable material and design for this application we have analyzed the above approaches thoroughly. The majority of them were disregarded due to different reasons, such as small aperture, bulky construction, high driving voltage, low speed, etc. We realized that the most suitable class of devices for our purpose is liquid crystal related. For the development of a light deflector we have chosen the concept of liquid crystal microprism arrays (LCMPAs), which excel in large aperture, sheet-like shape, high optical quality, low driving voltage, high pointing speed, and broadband operation. The combination of the optical birefringence effect and a periodic prism deviation structure is the core of this design. The deflection angles of ordinary ray (*O*-ray) and extraordinary ray (*E*-ray) in this configuration are distinctly different and switching between them can be carried out by changing polarization direction of light before entering this device. Regarding the polarization modulator, a 90° twisted nematic (TN) cell operating in the Mauguin mode was employed.

In this paper, we demonstrate a novel liquid crystal beam steering screen which consists of two cascaded identical layers

of 90° TN LC cell/LCMPA pairs. The working principle, fabrication, and test results of the steering screen are also presented. The experimental results show that the liquid crystal beam steering screen is suitable for broadband wavelength operation with low dispersion and low residual undesired beam intensity of orthogonal polarization.

## 2. CONFIGURATION AND PRINCIPLE OF THE LIQUID CRYSTAL BEAM STEERING SCREEN

The beam steering screen consists of a 90° TN LC cell and a passive birefringent LCMPA, which are used as the polarization modulator and light beam deflector, respectively. The 90° TN LC cell has two states as a polarization modulator. When a voltage is applied, it works as a transparent plate and the polarization state remains unchanged. When no voltage is applied it operates as a polarization rotator in the waveguide property mode and polarization rotated by 90°. In order to meet broadband demand, the 90° TN LC cell works under the Mauguin condition to ensure wavelength independence. As birefringent materials such as calcite, rutile, and quartz are difficult to be made in large size at low cost, we selected LC for our birefringent prism array; this has a large range of birefringence, and it is also a mature commercial product and has the potential to be fabricated in larger sizes. The proposed LCMPA structure schematic diagram (not drawn to scale) is shown in Fig. 1, where the birefringent LC prism is formed between the glass substrate and the polymethyl methacrylate (PMMA) micro prism-array (MPA) substrate. It can deviate the *O*-ray and *E*-ray in different directions. The optical axis is defined as the long axis of the liquid crystal molecule in the voids as labeled in Fig. 1.

Figure 2 shows the working principle of the beam steering screen. Only several units of prism cross section are depicted to illustrate the principle. The LC director of the 90° TN LC cell closest to the incident light is parallel to the incident light polarization; the optical axis of the passive LCMPA is parallel to the rear layer LC director of the 90° TN LC cell to satisfy the condition that output linear polarization of light from the TN cell is either parallel or perpendicular to the optical axis of the LCMPA. The two operating states are illustrated in Fig. 2. When the operating voltage  $V = 0$ , the output light is deflected to other direction with its polarization rotated by 90°, as shown in Fig. 2(a). When the operating voltage is applied, the incident linearly polarized light propagates through the two devices and keeps continuing in the original direction

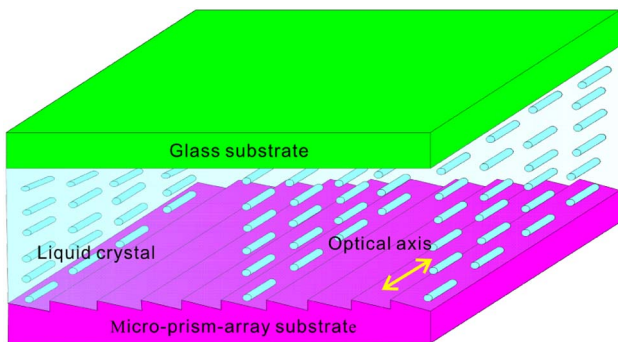


Fig. 1. Schematic of the proposed LCMPA device.

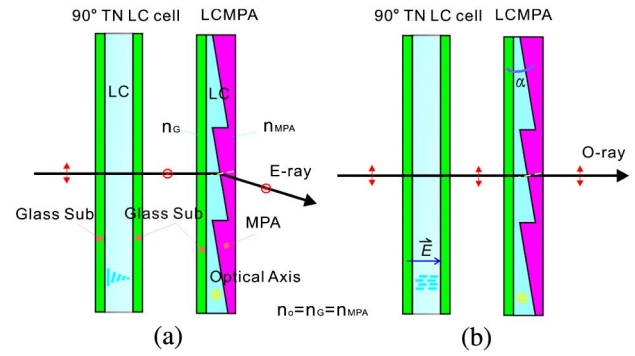


Fig. 2. Schematic illustration of the beam steering screen. (a) The 90° TN LC cell without applied voltage. (b) The 90° TN LC cell with applied voltage.

with no change in its polarization state, as shown in Fig. 2(b). Double refraction created by the birefringent LCMPA is utilized in order to provide two different deflection angles.

A pair of antiparallel identical steering screens for use in an autostereoscopic display is illustrated in Fig. 3. In this case one incident light beam can be steered in three directions by controlling two TN LC cells. In the absence of the applied voltage, the linearly polarized light transmitted by the 90° TN LC cell has its polarization rotated by 90°. When linearly polarized light passes through a two-layer cascaded beam steering screen system, there are four output conditions, as illustrated in Fig. 3. However, since both prism layers have the same facet angle, there are only three different output directions as the deflection in one direction is exactly canceled out by a second deflection in the opposite direction. Additionally, the output light polarization state and deflection direction corresponding to the operation states of the two TN LC cells are listed in Fig. 3.

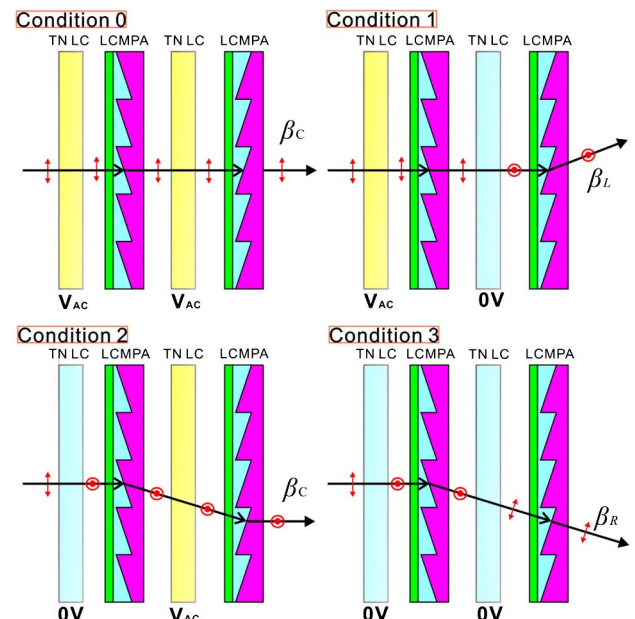


Fig. 3. Schematic illustration of the proposed cascaded steering screens.

Under condition 1, the light beam is deflected to the left direction by angle  $\beta_L$ . It continues to propagate without refraction and deviation under conditions 0 and 2 (angle  $\beta_C$  in Fig. 3). Finally, under condition 3, the light is deflected to the right side by angle  $\beta_R$ . Assuming for the sake of simplification that the refractive indices of glass, the prism array, and the ordinary refractive index of liquid crystal have all the same value, the deviation angles  $\beta_L$  and  $\beta_R$  can be calculated as

$$\beta_L = \arcsin \left( n_o * \left( \arcsin \left( \frac{n_e * \sin \alpha}{n_o} \right) - \alpha \right) \right) \approx (\Delta n) \alpha, \quad (1)$$

$$\beta_C = 0, \quad (2)$$

$$\beta_R = \arcsin \left( n_o * \sin \left( \alpha - \arcsin \left( \frac{n_e * \sin \alpha}{n_o} \right) \right) \right) \approx (-\Delta n) \alpha, \quad (3)$$

where  $\Delta n = n_e - n_o$ , is the birefringence of the LC;  $n_o$  and  $n_e$  are ordinary and extraordinary refractive indices, respectively, of the LC; and  $\alpha$  is the apex angle of the prism array.

According to Eqs. 1–3, the steering angle is determined by the apex angle of the prism and the birefringence of the LC. For larger deflection angles, increasing the apex angle of the prism or the birefringence of the LC separately or together are the commonly used methods. The limited birefringence  $\Delta n$  of the LC and the total internal reflection at the LC-to-MPA interface are the two main limitations for the larger deviation angles. However, the larger deviation angle can be achieved by cascading layers of the LCMPA. For example, if two layers of the same LCMPA are cascaded in parallel, the output steering angle will be doubled.

### 3. FABRICATION

The 75 mm × 75 mm LCMPA sample fabricated in our laboratory is shown in Fig. 4. The proposed LCMPA is composed of a top MPA substrate made of PMMA and a bottom glass substrate, and sandwich LC in the middle. The key process in the fabrication of the LCMPA is the LC alignment in the prismatic voids. The optical axis parallel to the prism pattern is adopted in our case as it is much easier to obtain than the perpendicular alignment. Conventional rubbing treatment is used for the glass substrate. However, it is unsuitable for a non-flat MPA substrate, and photoalignment is thus employed on its surface as the advanced technique for this case. The benefits

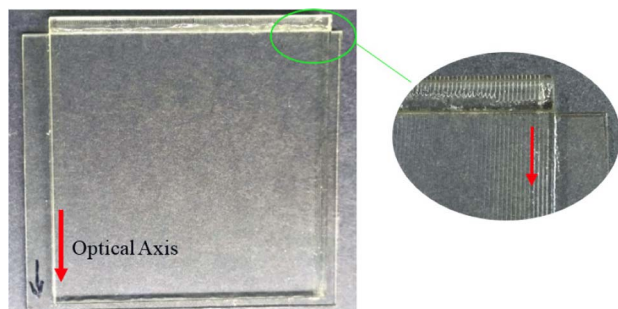


Fig. 4. 75 mm × 75 mm LCMPA samples.

of photoalignment that without causing rubbing trace, electric charging, and noncontact technology provide effective control of the basic anchoring parameters: easy orientation axis, pretilt angle, and anchoring energy [15]. Therefore, the combination of rubbing (glass substrate) and photoalignment (MPA substrate) are used to enhance the LCMPA structure. The LC alignment direction is the optical axis indicated by the red arrow in Fig. 4. The thickness of the LCMPA is only 2.9 mm including a 1.8 mm MPA substrate and 1.1 mm glass substrate.

The detailed fabrication processing of the proposed LCMPA is presented as follows. The azobenzene sulfuric dye SD1 [16] was dissolved in 2-ethoxyethanol with the concentration of 1 wt. %. A solution that had been filtered to 0.45 μm particle size was spin-coated on a well-cleaned MPA substrate at 800 rpm for 5 s then at 3000 rpm for 30 s. The SD1 coated on the MPA was baked at 60° in an oven for 5 min. Then, the surface was irradiated with a linearly polarized 450 nm blue light source for 30 min. Blue light exposure induced an effective reorientation of SD1 molecules, which was perpendicular to the polarization direction of activating light. The SD1 molecules used as the orientation layer in the voids provide LC alignment comparable to that of rubbed polyimide film [17]. The next stage was the preparation of the glass substrate. It was spin-coated with polyimide, baked in the oven at 230° for 30 min for the imidization of polyimide, and then unidirectionally rubbed. Finally, the two substrates were combined in such a manner that the axes of alignment induced on these two substrates were parallel to each other. Afterward, the cell was glued and then its prismatic voids were filled with nematic LC by capillary forces.

For preparation of the steering device, we used a commercially available MPA substrate with a thickness 1.8 mm, apex angle 11°, and facet pitch 0.508 mm. Next, LC parameters were optimized based on the requirement of a 0.952° steering angle for the autostereoscopic system. Substituting deflection angle  $\beta = 0.952^\circ$ , apex angle  $\alpha = 11^\circ$ , and  $n_o = 1.5$  in Eqs. 1–3, the other two parameters of LC,  $\Delta n = 0.0857$  and  $n_e = 1.5857$ , are obtained. The ordinary refractive index  $n_o$  equal to the refractive index of glass and PMMA is to ensure the middle beam in the original direction and the left–right beam symmetry after refraction. The MLC-7800-000 nematic LC from the Merck Company with  $\Delta n = 0.0854$  at 589 nm is selected. Its birefringence  $\Delta n$  decreases toward the longer wavelengths, as shown in Fig. 5 (left y-axis). The relationship between the calculated deviation angle and wavelength is plotted in Fig. 5 (right y-axis). The two curves demonstrate the same variation trend. It indicates that the major difference of deviation angle with wavelength is due to the dispersion of the LC material.

## 4. EXPERIMENTAL RESULTS AND DISCUSSION

### A. Optical Performance of LCMPA

To estimate the optical performance of the LCMPA, several preliminary experiments are implemented using a wavelength-tunable laser. Figure 6 shows a schematic diagram of the experimental setup used for testing the steering angle and dispersion of the LCMPA device. A tunable laser is used as the light source and its output passes through a polarizer

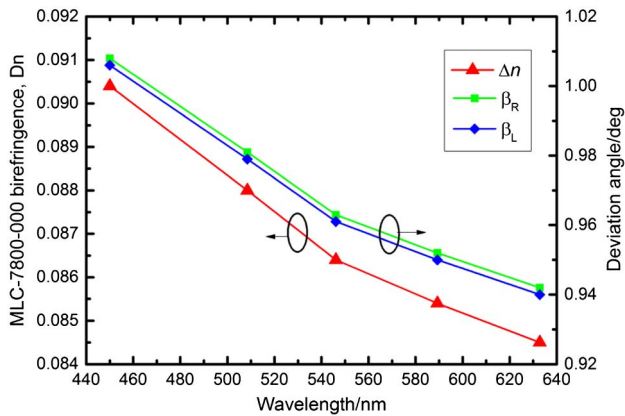


**Fig. 5.** MLC-7800-000 birefringence and deviation angle as a function of wavelength.

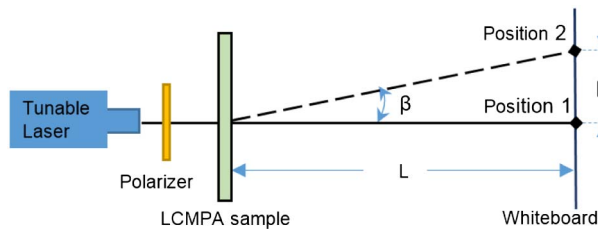


**Fig. 6.** Schematic diagram of the experimental setup for measuring a single layer of the steering screen.

plate that acts as an optical modulator and allows only light with a specific linear polarization to pass through it. A whiteboard, which is used to record the beam position, is placed at a known distance. The developed LCMPA sample is inserted behind the polarizer with the glass substrate side toward the light source because the plane surface as the incidence plane is effective for reducing the refraction, scattering, and residual light diffraction.

The laser beam lands on the whiteboard at 10.2 cm when without the LCMPA sample. When the LCMPA sample is placed in the optical path, the incident light whose polarization is perpendicular to the optical axis of the LCMPA reaches the whiteboard at its original position of 10.2 cm. When the incident light polarization is parallel to the optical axis of the LCMPA, it is deflected to a new position of 9.4 cm on the whiteboard (Fig. 7). The viewing distance between the LCMPA and whiteboard is 47.5 cm. The deviation angle can be calculated by  $\beta = \arctan(D/L)$ , where  $D$  is the distance between two light spots and  $L$  is the observation distance between the whiteboard and LCMPA. According to the above equation, the measured deviation angle is  $0.964^\circ$ . Compared to the designed deviation angle of  $0.952^\circ$ , the error between the experimental and design value is less than 1.26%. The reason for the difference between the theoretical and experiment values may be due to the structural variation in fabrication.

Three primary wavelengths (450, 546, and 632 nm) are selected for measuring the dispersion, which are matched to

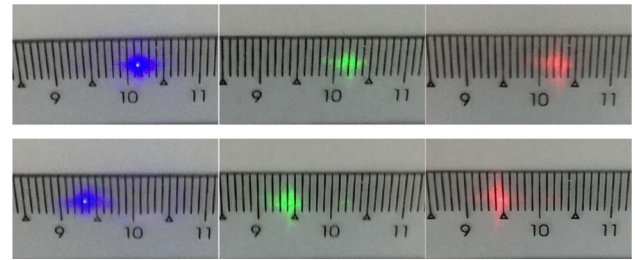


**Fig. 7.** Record of laser beam positions on the whiteboard when the incident linear polarization is parallel (top) or perpendicular (bottom) to the optical axis of LCMPA.

the peak transmission wavelengths of the color filters in a liquid crystal display. Figure 7 is a record of the laser beam position on the whiteboard when the incident light polarization is parallel or perpendicular to the optical axis of the LCMPA. The experimental results show that the three colored light spots are located so close to each other under the same condition so that the distance caused by dispersion is less than 2 mm. The steering distances between the light spots of orthogonal polarization of blue, green, and red spots are  $\sim 0.82$ ,  $\sim 0.8$ , and  $\sim 0.78$  cm (the readout of spot position was determined using the Microsoft paint and the accuracy of the readout is about  $\pm 30 \mu\text{m}$ ). This means that corresponding deviation angles are  $0.989^\circ$ ,  $0.964^\circ$ , and  $0.941^\circ$  and thus light dispersions are 2.6% ( $= (0.989^\circ - 0.964^\circ) / 0.964^\circ$ ) and 2.4% ( $= ((0.964^\circ - 0.941^\circ) / 0.964^\circ)$ ) with the 546 nm as reference. When the viewing screen is at 1200 mm, the distance between the red spot and blue spot caused by dispersion on the whiteboard is 0.52 mm ( $= \tan(0.989^\circ - 0.964^\circ) \times 1200 \text{ mm}$ ). The closer the viewing screen, the smaller is the dispersion. This result is consistent with the theoretical calculations showing that the steering angle decreases as the wavelength increases.

In Fig. 8, the deviation angle with an incidence angle varying from  $-30^\circ$  to  $+30^\circ$  with an interval of  $5^\circ$  at three wavelengths is displayed. From the plots of the theoretical and experimental results it is apparent that the deviation angle increases with the increasing incidence angle regardless of the wavelength dispersion. The experimental results are close to

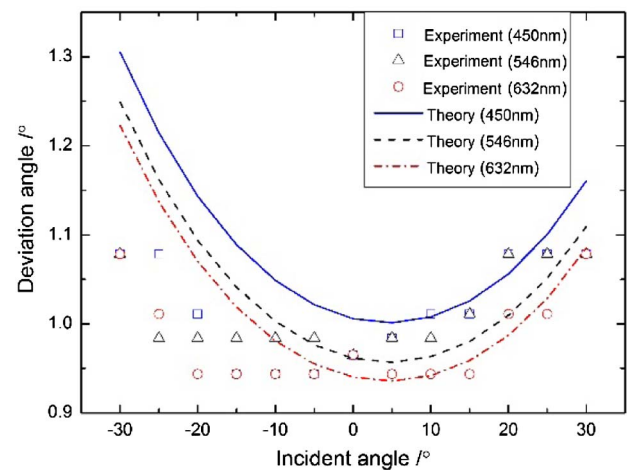


**Fig. 8.** Experiment deviation angle varied in large incident angle.

the theoretical values. The difference between the theoretical and experimental results is due to the theoretical calculations being made assuming ideal conditions; the dispersion of each layer of material is not taken into consideration. With the incidence angle from  $-30^\circ$  to  $+30^\circ$ , the experimental deviation angles are in the range of  $0.936^\circ$ – $1.078^\circ$ . This means, there is around 11.8% ( $= (1.078 - 0.964) / 0.964$ ), 2.38 mm ( $= \tan(1.078^\circ - 0.964^\circ) \times 1200$  mm) distance shift at 1200 mm on the viewing screen at  $\pm 30^\circ$  incident light input compared to the normal incidence. The measured results indicate that the LCMPA device is suitable for a large variation in input angles; it only gives a beam deviation difference of 11% with a  $\pm 30^\circ$  change in incident angle.

Finally we consider response time of the proposed screen. Because the LCMPA is a passive device, the system drive control and speed are dependent on the TN LC cells. Our in-house made  $75 \text{ mm} \times 75 \text{ mm} \times 2.2 \text{ mm}$  ( $W \times L \times T$ ) TN LC cell needed about 10 V operation voltage and demonstrated quite slow response time  $\sim 100$  ms. As is well known, the response time of the TN LC cell can be decreased to the range of milliseconds by reducing thickness and optimizing properties of the LC [18]. However, this cell will not work in the Mauguin regime anymore and so its response will be wavelength dependent. To keep the advantage of thick TN cells, in the future we plan to replace conventional nematic LC by dual-frequency nematic LC, which gives fast electro-optic response (in the range of several milliseconds) even in the Mauguin mode [19].

## B. Two-Layer Cascade of LCMPAs

A two-layer cascaded steering screen was designed for use in a new design of autostereoscopic display where the light output from the display screen should be sequentially directed in three different discrete directions. The second LCMPA is antiparallel to the first LCMPA (as illustrated in Fig. 3) so that the position of the original light spot will be in the middle of the three steered spots. Finally, a total thickness about 10.2 mm for the compressive beam steering system is achieved. In order to automatically control the light spot steering from condition 0 to condition 3, an integrated field programmable gate array system for the TN LC cell driver was designed. The experimental setup for measuring the cascaded system is shown in Fig. 9.

A single-wavelength laser of 532.8 nm was used as a light source to measure the steering angle. The light beam was sequentially steered to three different positions on the whiteboard. The positions of three static light spots at three statuses are shown in Fig. 10. The light beam arrived at the original position on the whiteboard at condition 2, whose steering angle was defined as  $0^\circ$  for reference, as shown in the middle photograph of Fig. 10. To easily observe the dynamic beam steering, a video was recorded, as shows the Visualization 1 in Fig. 10. At conditions 1 and 3, the laser beams were steered to the left and right with steering angles  $-0.9548^\circ$  ( $= \arctan(-1.75 \text{ cm} / 105 \text{ cm})$ ) and  $0.9548^\circ$ , respectively, as shown in the top and bottom of Fig. 10. The same left and right steering angle is required in the stereoscopic display system. The result shows that the measured steering angle  $0.9548^\circ$  of two cascaded layers is close to the angle of  $0.964^\circ$  of one single layer LCMPA. There is about 1%

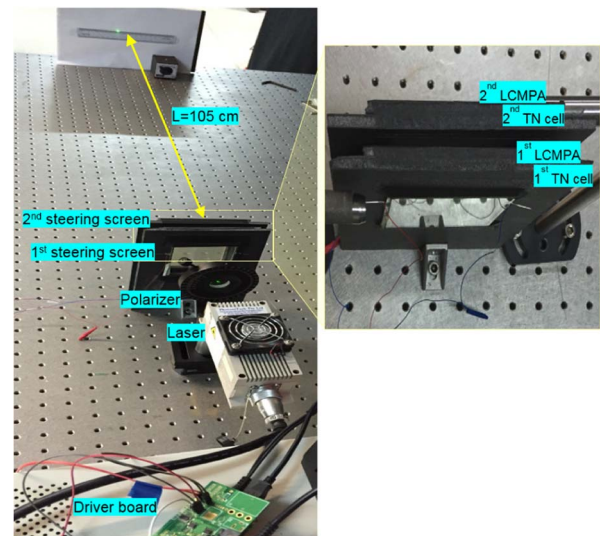


Fig. 9. Experimental setup for the cascaded steering screen system.

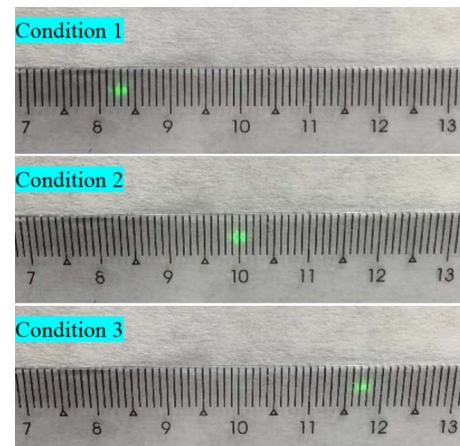


Fig. 10. Beam steering spots land on the whiteboard under three conditions. (See Visualization 1.)

( $= (0.964 - 0.9548) / 0.964$ ) difference, which might be due to the system assembly. In this way the two-layer cascaded beam steering system can be used to steer light from the entire screen light to the three directions required.

When the desired polarization light spot reaches the whiteboard, the undesired orthogonal polarization light spot is also visible. This is referred to as the polarization residual spot and its effect is important as it causes cross talk in the display. The polarization residual contrast ratio is defined as the ratio of the desired polarization output to its orthogonal nondesired component residual spot. For this two-layer cascaded system, there are two residual light spots at one condition. The power of the light spot was measured by a Konica Minolta CL-500A spectrophotometer. The measured residual polarization spot contrast is listed in Table 1. The maximal residual spot contrast ratio is 2.0% at condition 1, which is lower than that of a diffractive wave plate [5]. Although these are initial experimental devices, the performances of the LCMPA and  $90^\circ$  TN LC cell are

**Table 1. Measured Residual Light Spot Contrast Ratio of Two-Layer Cascaded Steering Screen System**

Position (cm)	Cond. 0 (%)	Cond. 1 (%)	Cond. 2 (%)	Cond. 3 (%)
1 (at 8.25)	100.0	2.0	1.2	100.0
2 (at 10.0)	1.0	100.0	100.0	1.1
3 (at 11.75)	1.6	0.9	1.9	0.6

sufficiently good to meet the requirements of our developed autostereoscopic display system.

## 5. CONCLUSIONS

In this paper we have demonstrated a two-layer cascaded beam steering screen system using 75 mm × 75 mm LCMPAs and 90° TN LC cells. The system automatically steers the light beam to three designed directions (−0.95°, 0°, and +0.95°) in sequence by an integrated drive controller. The dispersion mainly caused by the LC material is about 2.6%, which means that the dispersion of the LCMPA is sufficiently low for it to be ignored for close viewing distances in 3D display application [20]. The difference of the steering angle is about 11.8% at 30° oblique incidence compared to the normal incidence. Moreover, the undesired residual polarization intensity of the beam was less than 2%, which is sufficient for our initial prototype.

The developed steering screen system has large size, thin compact structure, requires only simple fabrication, and controls broadband light with a precise steering angle. It was demonstrated that the light from a large aperture source, such as a display screen, can be steered to the target directions with an acceptably small error. Such a device has many potential applications in photonic and displays, particularly in the area of 3D display. However, for the latter application, the problem of slow response of the device is required to be solved. We solved this problem with the use of dual-frequency LC in the TN cells operating in the Mauguin mode. By this way, we intend to keep low dispersion of the steering screen and gain faster response time approximating the value required for the 3D display (~1 ms) [14].

**Funding.** National Research Foundation Singapore (NRF) (NRF-CRP11-2012-01).

## REFERENCES

1. A. Tuantranont, V. M. Bright, J. Zhang, W. Zhang, J. A. Neff, and Y. C. Lee, "Optical beam steering using MEMS-controllable microlens array," *Sens. Actuators A* **91**, 363–372 (2001).
2. M. H. Kiang, O. Solgaard, K. Y. Lau, and R. S. Muller, "Electrostatic combdrive-actuated micromirrors for laser-beam scanning and positioning," *J. Microelectromech. Syst.* **7**, 27–37 (1998).
3. O. T. V. Ramm and S. W. Smith, "Beam steering with linear arrays," in *Proceedings of IEEE Conference on Transactions on Biomedical Engineering* (IEEE 1983), pp. 438–452.
4. Y. J. Lin, K. M. Chen, and S. T. Wu, "Broadband and polarization-independent beam steering using dielectrophoresis-tilted prism," *Opt. Express* **17**, 8651–8656 (2009).
5. S. V. Serak, R. S. Hakobyan, S. R. Nersisyan, N. V. Tabiryan, T. J. White, T. J. Bunning, D. M. Steeves, and B. R. Kimball, "All-optical diffractive/transmissive switch based on coupled cycloidal diffractive waveplates," *Opt. Express* **20**, 5460–5469 (2012).
6. N. V. Tabiryan, S. R. Nersisyan, D. M. Steeves, and B. R. Kimball, "The promise of diffractive waveplates," *Opt. Photon. News* **21**(12), 41–45 (2010).
7. H. Chen, Y. Weng, D. Xu, N. V. Tabiryan, and S. T. Wu, "Beam steering for virtual/augmented reality displays with a cycloidal diffractive waveplate," *Opt. Express* **24**, 7287–7298 (2016).
8. J. Kim, C. Oh, M. N. Miskiewicz, S. Serati, and M. J. Escuti, "Demonstration of large-angle nonmechanical laser beam steering based on LC polymer polarization gratings," *Proc. SPIE* **8052**, 80520T (2011).
9. C. T. DeRose, R. D. Kekatpure, D. C. Trotter, A. Starbuck, J. R. Wendt, A. Yaacobi, M. R. Watts, U. Chettiar, N. Engheta, and P. S. Davids, "Electronically controlled optical beam-steering by an active phased array of metallic nanoantennas," *Opt. Express* **21**, 5198–5208 (2013).
10. P. F. McManamon, P. J. Bos, M. J. Escuti, J. Heikenfeld, S. Serati, H. K. Xie, and E. A. Watson, "A review of phased array steering for narrow-band electrooptical systems," *Proc. IEEE* **97**, 1078–1096 (2009).
11. J. R. Lindle, A. T. Watnik, and V. A. Cassella, "Efficient multibeam large-angle nonmechanical laser beam steering from computer-generated holograms rendered on a liquid crystal spatial light modulator," *Appl. Opt.* **55**, 4336–4341 (2016).
12. N. R. Smith, D. C. Abeysinghe, J. W. Haus, and J. Heikenfeld, "Agile wide-angle beam steering with electrowetting micropisms," *Opt. Express* **14**, 6557–6563 (2006).
13. Y. B. Xie, W. Q. Wang, H. Y. Chen, A. Konneker, B. L. Popa, and S. A. Cummer, "Wavefront modulation and subwavelength diffractive acoustics with an acoustic metasurface," *Nat. Commun.* **5**, 1–5 (2014).
14. X. Zhang, H. Wang, and P. A. Surman, "A spatial-temporal multiplexing autostereoscopic display for demonstration of a super multiview 3D," (in preparation).
15. O. Yaroshchuk and Y. Reznikov, "Photoalignment of liquid crystals: basics and current trends," *J. Mater. Chem.* **22**, 286–300 (2012).
16. H. Akiyama, T. Kawara, H. Takada, H. Takatsu, V. Chigrinov, E. Prudnikova, V. Kozenkov, and H. Kwok, "Synthesis and properties of azo dye aligning layers for liquid crystal cells," *Liq. Cryst.* **29**, 1321–1327 (2002).
17. A. D. Kiselev, V. Chigrinov, and D. D. Huang, "Photoinduced ordering and anchoring properties of azo-dye films," *Phys. Rev. E* **72**, 061703 (2005).
18. V. G. Chigrinov, *Liquid Crystal Devices: Physics and Applications* (Artech House, 1999).
19. A. B. Golovin, O. P. Pishnyak, S. V. Shiyonovskii, and O. D. Lavrentovich, "Achromatic linear polarization switch for visible and near infrared radiation based on dual-frequency twisted cell," *Proc. SPIE* **6135**, 61350E (2006).
20. F. L. Kooi and A. Toet, "Visual comfort of binocular and 3D displays," *Displays* **25**, 99–108 (2004).